



**HAL**  
open science

## Lithium in Portland cement clinker: absence of evidence is not evidence of absence

Vincent Thiéry, Nicolas Nuns

► **To cite this version:**

Vincent Thiéry, Nicolas Nuns. Lithium in Portland cement clinker: absence of evidence is not evidence of absence. *Advances in Cement Research*, 2025, pp.1-6. 10.1680/jadcr.24.00229 . hal-05101639

**HAL Id: hal-05101639**

**<https://imt-nord-europe.hal.science/hal-05101639v1>**

Submitted on 6 Jun 2025

**HAL** is a multi-disciplinary open access archive for the deposit and dissemination of scientific research documents, whether they are published or not. The documents may come from teaching and research institutions in France or abroad, or from public or private research centers.

L'archive ouverte pluridisciplinaire **HAL**, est destinée au dépôt et à la diffusion de documents scientifiques de niveau recherche, publiés ou non, émanant des établissements d'enseignement et de recherche français ou étrangers, des laboratoires publics ou privés.

1 **R3 version**

2 **Lithium in Portland cement clinker: absence of evidence is not evidence of absence**

3  
4 Vincent THIÉRY<sup>1,2\*</sup>, Nicolas NUNS<sup>3</sup>

5 <sup>1</sup> IMT Nord Europe, Institut Mines-Télécom, Centre for Materials and Processes, F-59000

6 Lille, France

7 <sup>2</sup> Univ. Lille, Institut Mines-Télécom, LGCgE – Laboratoire de Génie Civil et

8 géoEnvironnement, F-59000 Lille, France

9 <sup>3</sup>Univ Lille, CNRS, INRAE, Cent Lille, Univ Artois, FR 2638,IMEC Inst Michel E, F-59000

10 Lille, France

11 \* corresponding author, vincent.thiery@imt-nord-europe.fr

12 Vincent THIÉRY: 0000-0002-1384-6000

13 **Abstract**

14 Lithium is a challenging element to analyse in mineral matrixes. The very low energy (54 eV)  
15 of its X-ray emission line makes it almost impossible to analyse by common methods such as  
16 energy dispersive spectroscopy. Hence, its localisation within cementitious phases is poorly  
17 known. Based on glow-discharge mass spectrometry (GD-MS) and time-of-flight secondary  
18 ion mass spectrometry (ToF-SIMS), the present paper shows for the first time the repartition  
19 of Li at the scale of a microstructure of clinker with a 200 nm lateral resolution. Li is  
20 correlated to both Al and Fe in the interstitial phase, but also to Mg in periclase.

21 **Keywords**

22 Lithium, Portland cement clinker, ToF-SIMS, microstructure, microscopy

23

## 24 **1 Introduction**

25 “*Absence of evidence is not evidence of absence*” is a quote from the famous astronomer Carl  
26 Sagan (1934-1996), highlighting a deep reflection about, according to (Feres and Feres,  
27 2023), the “*logical fallacy where a hypothesis is assumed to be true or false before being*  
28 *scientifically and satisfactorily investigated*”. While all those implications are way beyond the  
29 topic of the present article, the above quote fits well to the quest of Li in cementitious  
30 materials.

31 Lithium ( $Z=3$ ) is a light element widely used in the so-called Li-ion batteries, but it also  
32 covers a wide range of applications, from medicine to treat bipolar disorder (Jope, 1999) to  
33 lubricant in grease (Yonggang and Jie, 1998). Within the framework of its use in batteries, Li-  
34 bearing minerals and battery components are gaining interest in their microanalysis, since Li  
35 is complex to analyse using traditional materials science analytical devices such as energy  
36 dispersive spectroscopy (Hovington *et al.*, 2016; Grew, 2020; Thiéry and Bou Farhat, 2023)

## 37 **2 Lithium in cementitious materials**

38 Li has very specific uses in cementitious materials, as described below, but it is also present  
39 naturally in raw materials and fuels used in the burning of Portland cement clinker (PCC).

### 40 *2.1 Li in the raw feed*

41 Considering that the main part of the raw feed of cement clinker consists of a mixture of clay  
42 and limestone, which are natural materials, Li is likely to be present. Indeed, although the raw  
43 mix consists of sedimentary rocks where typical Li-bearing micas are unlikely to be present,  
44 the natural presence of Li in muscovite cannot be excluded (Korbel, Filippova and Filippov,  
45 2023; Sulcek, Marler and Fechtelkord, 2023). Raw feed involving other types of rocks than

46 sedimentary ones, typically metamorphic rocks, are prone to a higher muscovite content  
47 (Korkmaz and Hacifazlıoğlu, 2024).

## 48 2.2 *Li in alternative fuels*

49 Alternative fuels are widespread in cement plant in order to burn various wastes (Aranda  
50 Usón *et al.*, 2013; Rahman *et al.*, 2015). They can be both solid or liquid. Although  
51 environmental policies strongly promotes the recycling of domestic batteries, it cannot be  
52 excluded to find them in municipal solid waste (MSW) (Kayla Kilgo *et al.*, 2022).

## 53 3 Analytical challenges of Li in cementitious materials

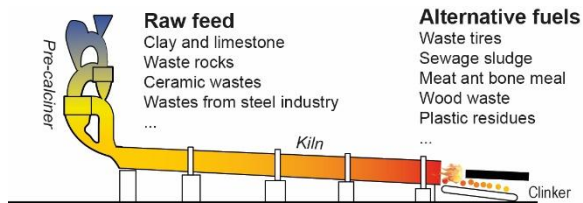
54 Like in any inorganic material in Earth or materials sciences, Li is elusive and tricky to  
55 analyse in-situ (Thiéry and Bou Farhat, 2023). However, in the very specific case of  
56 cementitious materials, the analysis is made even more difficult considering their hydrous  
57 state, porosity, beam sensitivity and chemical variations at the micrometre scale (Diamond,  
58 2004; Scrivener, 2004; Stutzman, 2004, 2012; Scrivener *et al.*, 2016; Thiéry, Trincal and  
59 Davy, 2017).

### 60 3.1 *Is Li present in cementitious materials?*

61 Prior to describing analytical possibilities to obtain qualitative or quantitative data for Li in  
62 those materials, it is worth recalling why this element is likely to be present. In the raw feed  
63 (Figure 1), clay and limestone are natural sources of Li. The Clarke (average content of an  
64 element in the continental crust) for Li is estimated at ca. 20 ppm (Teng *et al.*, 2004), which,  
65 of course, is likely to exhibit significant variations across the various geological layers.  
66 Moreover, Li seems to be almost absent from limestones, but rather concentrated in shales  
67 (Horstman, 1957). For example, Australian shales have yielded up to 109 ppm Li (Teng *et al.*,  
68 2004), but limestone are down to 5 ppm (Horstman, 1957). However, the range of variation is  
69 really wide and highly dependent on the lithological type (Chan, Leeman and Plank, 2006).

70 Indeed, in sedimentary rocks, Li is associated with clay minerals (hence its presence in shales  
71 rather than in carbonates) (Zhao, Wang and Cheng, 2023).

72



73

74 *Figure 1. Schematic view of a Portland cement kiln and associated sources of Li*

### 75 3.2 Analytical methods giving access to Li analysis

76 **Laser ablation with inductively coupled plasma mass spectrometry (LA-ICP-MS)** is  
77 widely used in Earth sciences but not so common in cement and concrete research (Decker *et*  
78 *al.*, 2021; Kleiner *et al.*, 2022). Although it yields compositional information for virtually the  
79 whole periodic table (including isotopes) down to the ppb level, the ablation crater, typically  
80 100 micrometres in diameter, is way too large for analysis at the microscale.

81 **Laser-induced breakdown spectroscopy (LIBS)** can yield interesting results for Li analysis  
82 in solids (Gallot-Duval *et al.*, 2024). However, as for LA-ICP-MS described above, the  
83 analytical spots can in some cases exceed the size of crystals to be analysed in clinker  
84 (Sweetapple and Tassios, 2015), although recent developments in the technique allow to  
85 produce ablation craters around 5 micrometers in diameter (Berthou *et al.*, 2024).

86 **Time of flight secondary ion mass spectrometry (ToF-SIMS)** is a surface analysis  
87 technique where the sample is bombarded with short pulses of primary ions. Then secondary  
88 ions generated are collected from the first nanometers of the sample via a time of flight  
89 analyser. A spectra is then obtained with characteristic peaks of elementary and molecular  
90 ions. (Penen *et al.*, 2022). By focusing and scanning the primary ion gun, secondary ions can

91 be images with a lateral resolution up to 200 nm. This technique allows the analysis of all  
92 elements with a high sensitivity (ppm-ppb). However, it does not provide a quantitative  
93 estimation of the composition due to the variability of the probability of ionisation from one  
94 sample to another. It had been applied to the study of Li behaviour in concrete suffering from  
95 alkali-silica reaction (Leemann *et al.*, 2014, 2015; Bernard and Leemann, 2015).

### 96 3.3 Challenges in SEM-EDS and electron microprobe (WDS)

97 Although those challenges have recently been discussed (Hovington *et al.*, 2016; Thiéry and  
98 Bou Farhat, 2023), the main points will be briefly recalled here. Energy-dispersive  
99 spectroscopy (EDS, or EDX) is routinely used as an analytical tool under the SEM (Georget,  
100 Wilson and Scrivener, 2021), both as individual points or as chemical maps.

101 The  $K\alpha$  band of Li is located at 54 eV, belonging to the “ultra-soft” X-rays category. They are  
102 possible to analyse only using windowless detectors, which are not common under the SEM  
103 (Hovington *et al.*, 2016), or using very specific detectors in WDS (Polkonikov *et al.*, 2021).

### 104 3.4 Where is Li in Portland cement clinker?

105 In order to illustrate the above points of interest, the present study focuses on the simplest  
106 component of cement, namely Portland cement clinker. Indeed, it provides in itself enough  
107 complexity to illustrate future works related to the same topic.

108 Contrarily to glasses and ceramics in which the  $\text{Li}_2\text{O-CaO-SiO}_2$  system is well known (West,  
109 1978; Konar and Jung, 2020), scarce literature is available on the topic of Li incorporation in  
110 PCC phases. An experimental study carried out by (Woermann, Hahn and Eysel, 1979)  
111 revealed that Li is preserved during the formation of tricalcium silicate and can be  
112 incorporated up to 1,2 wt%  $\text{LiO}_2$  in this phase. During clinkerization, it is known that a minor  
113 amount of  $\text{Li}_2\text{O}$  lowers the melting temperature, hence promoting the formation of the  
114 interstitial phase (Bhatty, 1995; Kolovos, Tsvivilis and Kakali, 2002). At the microstructural

115 level, the incorporation of  $\text{Li}_2\text{O}$  in the raw feed of laboratory synthesized clinkers resulted in  
116 the transformation of the borders of  $\text{C}_3\text{S}$  in a mixture of  $\text{C}_2\text{S}$  and lime (Boháč *et al.*, 2022). In  
117 all examples,  $\text{Li}_2\text{O}$  was not quantified nor observed at the microstructural level.

118 Surrounding the calcium silicates in PCC, the so-called “interstitial phase” is a mixture of  
119 tetra-calcium aluminate ferrite ( $\text{C}_4\text{AF}$ ) with a brownmillerite structure (Colville and Geller,  
120 1971), and tricalcium aluminate ( $\text{C}_3\text{A}$ ). Only brownmillerite can accommodate Li in its  
121 structure (Mohamed *et al.*, 2022). Hence, according to the above review, it seems that Li can  
122 be present both in alite ( $\text{C}_3\text{S}$ ) and ferrite ( $\text{C}_4\text{AF}$ ), but this repartition has never been observed  
123 experimentally.

#### 124 **4 Materials and methods**

125 A sample of commercial Portland cement clinker was prepared for microscopy using common  
126 resin embedding and polishing procedure, using water-free lubricants (Thiéry, Dubois and  
127 Bellayer, 2022). To obtain the Li content of the sample, a raw chip of clinker was analysed  
128 using a Nu-Astrum glow discharge mass spectrometer (GD-MS). The sample was placed on a  
129 tantalum holder, within a Pin Cell cell type, under a constant flux of Ar, a glow discharge  
130 potential of 1 kV with a 3 mA sample current.

131 ToF-SIMS analysis were performed on a TOF.SIMS<sup>5</sup> machine from IONTOF equipped with a  
132 Bi primary ion source and with Cs and  $\text{O}_2$  for sputtering. Prior to the analysis, sample was  
133 etched with  $\text{O}_2$  sputter gun (2kV, 700nA) over an area of  $700 \times 700 \mu\text{m}^2$  during 5 minutes.  
134 This operation was performed in order to remove contamination induce during sample  
135 preparation. Then an analysis were performed in the center of the  $\text{O}_2$  crater over an area of  
136  $200 \times 200 \mu\text{m}^2$ . Bi primary ion gun was used in burst mode (6 pulses) in order to combine  
137 both a good lateral resolution and a correct mass resolution. Mass resolution obtain on this  
138 condition was 2000 at  $m/z = 40$  for  $\text{Ca}^+$ . Cycle time was  $70 \mu\text{s}$  and allowed us to obtain

139 masses up to 450 m/z. We chose 256 x 256 pixels for data acquisition and we cumulated 1000  
140 scans to have significant intensity for Li<sup>+</sup> secondary ions.

141

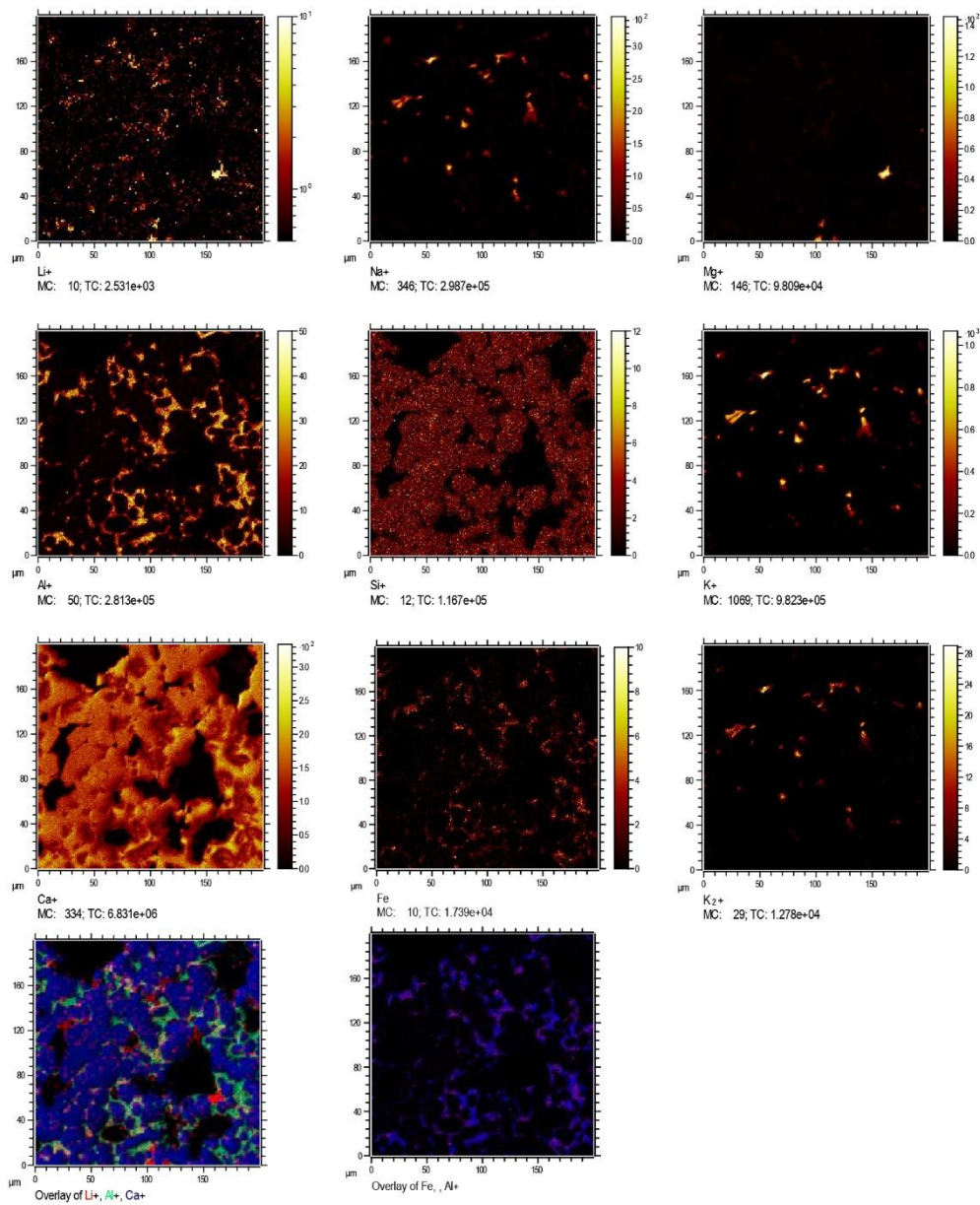
## 142 **5 Results and discussion**

143 GD-MS gives a Li content of 130 ppm. This is in good agreement with the very low content  
144 of the initial raw materials used in the making of clinker's raw feed (§ 3.1 above), but also  
145 showing an enrichment relatively to its natural content in the continental crust (Teng *et al.*,  
146 2004, 2008). The loss of volatiles during the clinkerization reactions (Kerton, 1993) might  
147 account for the concentration of Li during the firing of the raw feed.

148 The repartition of elements at the scale of the microstructure using ToF-SIMS is illustrated in  
149 **Erreur ! Source du renvoi introuvable.** The results are similar to what could have been  
150 obtained with a common EDS detector: chemical maps account for a representation of the  
151 traditional phases. For instance, the correlation between Ca and Si allows to locate the  
152 calcium silicates. Ca, Al and Fe, on the other hand, are located in the so-called interstitial  
153 phase, surrounding the calcium silicates. However, the interest of ToF-SIMS in this case is to  
154 show the presence of Li, for which several correlations can be made. While there seems to be  
155 a low concentration through the entire microstructure, higher amounts, directly correlated to  
156 Al and Fe in the interstitial phase, can be seen. This is in good agreement with the description  
157 of Li substitution in ferrites and brownmillerites structures (Panda, Hota and Choudhary,  
158 2023; Askarzadeh and Shokrollahi, 2024; Spanu *et al.*, 2024), which are classically  
159 considered as reference structures for phases from the interstitial phase of clinker. However,  
160 this had never been observed by ToF-SIMS mapping (or any other chemical map). Finally,  
161 the highest relative Li concentration in clinker is directly correlated to Mg only, implying the  
162 Mg-Li substitution in periclase MgO, which is a common (but not desirable) phase in clinker

163 (Song *et al.*, 2021). This substitution had already been described (Doman, Alper and McNally,  
 164 1968), and, interestingly, in the present case, there is no correlation with Al, while high  
 165 temperature substitution of  $\text{LiAlO}_2$  in the  $\text{MgO}$  lattice (Doman and McNally, 1973).

166



167

168 *Figure 2. ToF-SIMS elemental maps on a polished section of Portland cement clinker.*

169

170 ToF-SIMS hence proves itself as a really powerful tool to observe the repartition of elements  
171 such as Li within a cementitious matrix. This has already been shown for ASR mitigation  
172 (Bernard and Leemann, 2015), and in the present case it allows deciphering Li repartition in a  
173 complex matrix with a very low concentration (130 ppm). It gives perspectives for the  
174 characterization of Li-bearing products in cementitious matrix. Indeed, surface-finishing agent  
175 based on Li silicate are commonly used (Tung, Kitagaki and Yamakita, 2020; Song, Lu and  
176 Lai, 2021; Jansová *et al.*, 2023). While the effects on the water absorption and microstructure  
177 have been described, the mechanisms and the localization and nature of the Li hydrates within  
178 the cementitious matrix are unknown. In the same way, it is well known that Li has a positive  
179 effect for Portland cement setting (Witzleben, 2020), but once again, the nature and  
180 microstructure of Li-bearing hydrated cement paste is not known.

## 181 **6 Conclusions**

182 Techniques poorly used in cement science, such as GD-MS and ToF-SIMS, are currently  
183 almost the only ones yielding valuable results to quantify and localise Li in a cementitious  
184 material. Until now, the repartition of Li within the various clinker phases had never been  
185 observed. ToF-SIMS allowed us to locate its presence in the so-called interstitial phase as  
186 well as in periclase, at a very low concentration (130 ppm) in the sample.

187

## 188 **References**

- 189 Aranda Usón, A. *et al.* (2013) 'Uses of alternative fuels and raw materials in the cement industry as  
190 sustainable waste management options', *Renewable and Sustainable Energy Reviews*, 23, pp. 242–  
191 260. Available at: <https://doi.org/10.1016/j.rser.2013.02.024>.
- 192 Askarzadeh, N. and Shokrollahi, H. (2024) 'A review on synthesis, characterization and properties of  
193 lithium ferrites', *Results in Chemistry*, 10, p. 101679. Available at:  
194 <https://doi.org/10.1016/j.rechem.2024.101679>.
- 195 Bernard, L. and Leemann, A. (2015) 'Assessing the potential of ToF-SIMS as a complementary  
196 approach to investigate cement-based materials — Applications related to alkali–silica reaction',

- 197 *Cement and Concrete Research*, 68, pp. 156–165. Available at:  
198 <https://doi.org/10.1016/j.cemconres.2014.11.008>.
- 199 Berthou, W. *et al.* (2024) ‘Characterization of lithium phosphorus oxide thin film libraries by laser-  
200 induced breakdown spectroscopy imaging: A step towards high-throughput quantitative analyses’,  
201 *Spectrochimica Acta Part B: Atomic Spectroscopy*, 215, p. 106906. Available at:  
202 <https://doi.org/10.1016/j.sab.2024.106906>.
- 203 Bhatti, J.I. (1995) *Role of minor elements in cement manufacture and use*. Edited by P.C. Association,  
204 p. 40.
- 205 Boháč, M. *et al.* (2022) ‘The role of Li<sub>2</sub>O, MgO and CuO on SO<sub>3</sub> activated clinkers’, *Cement and*  
206 *Concrete Research*, 152, p. 106672. Available at: <https://doi.org/10.1016/j.cemconres.2021.106672>.
- 207 Chan, L.-H., Leeman, W.P. and Plank, T. (2006) ‘Lithium isotopic composition of marine sediments’,  
208 *Geochemistry, Geophysics, Geosystems*, 7(6). Available at: <https://doi.org/10.1029/2005GC001202>.
- 209 Colville, A.A. and Geller, S. (1971) ‘The crystal structure of brownmillerite, Ca<sub>2</sub>AlFeO<sub>5</sub>’, *Acta*  
210 *Crystallographica Section B*, 27(12), pp. 2311–2315. Available at:  
211 <https://doi.org/10.1107/S056774087100579X>.
- 212 Decker, M. *et al.* (2021) ‘LA-ICP-MS on hardened cement paste: laser-material interaction, signal  
213 formation and optimization of laser fluence’, *Materials and Structures*, 54(4), p. 144. Available at:  
214 <https://doi.org/10.1617/s11527-021-01736-4>.
- 215 Diamond, S. (2004) ‘The microstructure of cement paste and concrete—a visual primer’, *Cement and*  
216 *Concrete Composites*, 26(8), pp. 919–933. Available at:  
217 <https://doi.org/10.1016/j.cemconcomp.2004.02.028>.
- 218 Doman, R.C., Alper, A.M. and McNally, R.N. (1968) ‘Periclase solid solutions containing Li<sup>+1</sup> and R<sup>+3</sup>  
219 ions’, *Journal of Materials Science*, 3(6), pp. 590–595. Available at:  
220 <https://doi.org/10.1007/BF00757904>.
- 221 Doman, R.C. and McNally, R.N. (1973) ‘Solid solution studies in the MgO-LiAlO<sub>2</sub> system’, *Journal of*  
222 *Materials Science*, 8(2), pp. 189–191. Available at: <https://doi.org/10.1007/BF00550666>.
- 223 Feres, M. and Feres, M.F.N. (2023) ‘Absence of evidence is not evidence of absence.’, *Journal of*  
224 *applied oral science : revista FOB*, 31, p. ed001. Available at: [https://doi.org/10.1590/1678-7757-](https://doi.org/10.1590/1678-7757-2023-ed001)  
225 [2023-ed001](https://doi.org/10.1590/1678-7757-2023-ed001).
- 226 Gallot-Duval, D. *et al.* (2024) ‘Depth profile analysis and high-resolution surface mapping of lithium  
227 isotopes in solids using laser-induced breakdown spectroscopy (LIBS)’, *Spectrochimica Acta Part B:*  
228 *Atomic Spectroscopy*, 215, p. 106920. Available at: <https://doi.org/10.1016/j.sab.2024.106920>.
- 229 Georget, F., Wilson, W. and Scrivener, K.L. (2021) ‘edxia: Microstructure characterisation from  
230 quantified SEM-EDS hypermaps’, *Cement and Concrete Research*, 141, pp. 106327–106327. Available  
231 at: <https://doi.org/10.1016/j.cemconres.2020.106327>.
- 232 Grew, E.S. (2020) ‘The Minerals of Lithium’, *Elements*, 16(4), pp. 235–240. Available at:  
233 <https://doi.org/10.2138/gselements.16.4.235>.

- 234 Horstman, E.L. (1957) 'The distribution of lithium, rubidium and caesium in igneous and sedimentary  
235 rocks', *Geochimica et Cosmochimica Acta*, 12(1), pp. 1–28. Available at:  
236 [https://doi.org/10.1016/0016-7037\(57\)90014-5](https://doi.org/10.1016/0016-7037(57)90014-5).
- 237 Hovington, P. *et al.* (2016) 'Can we detect Li K X-ray in lithium compounds using energy dispersive  
238 spectroscopy?', *Scanning*, 38(6), pp. 571–578. Available at: <https://doi.org/10.1002/sca.21302>.
- 239 Jansová, K. *et al.* (2023) 'The influence of lithium silicate impregnation on the properties of surface  
240 layer of cementitious composites', *Journal of Physics: Conference Series*, 2568(1), p. 012004.  
241 Available at: <https://doi.org/10.1088/1742-6596/2568/1/012004>.
- 242 Jope, R.S. (1999) 'Anti-bipolar therapy: mechanism of action of lithium', *Molecular Psychiatry*, 4(2),  
243 pp. 117–128. Available at: <https://doi.org/10.1038/sj.mp.4000494>.
- 244 Kayla Kilgo, M. *et al.* (2022) 'Metal leaching from Lithium-ion and Nickel-metal hydride batteries and  
245 photovoltaic modules in simulated landfill leachates and municipal solid waste materials', *Chemical  
246 Engineering Journal*, 431, p. 133825. Available at: <https://doi.org/10.1016/j.cej.2021.133825>.
- 247 Kerton, C.P. (1993) 'Behaviour of Volatile Materials in Cement Kiln Systems', in R. Clift and J.P.K.  
248 Seville (eds) *Gas Cleaning at High Temperatures*. Dordrecht: Springer Netherlands, pp. 589–603.  
249 Available at: [https://doi.org/10.1007/978-94-011-2172-9\\_37](https://doi.org/10.1007/978-94-011-2172-9_37).
- 250 Kleiner, F. *et al.* (2022) 'Combined LA-ICP-MS and SEM-EDX analyses for spatially resolved major,  
251 minor and trace element detection in cement clinker phases', *Cement and Concrete Research*, 159, p.  
252 106875. Available at: <https://doi.org/10.1016/j.cemconres.2022.106875>.
- 253 Kolovos, K., Tsvivilis, S. and Kakali, G. (2002) 'The effect of foreign ions on the reactivity of the CaO–  
254 SiO<sub>2</sub>–Al<sub>2</sub>O<sub>3</sub>–Fe<sub>2</sub>O<sub>3</sub> system: Part II: Cations', *Cement and Concrete Research*, 32(3), pp. 463–469.  
255 Available at: [https://doi.org/10.1016/S0008-8846\(01\)00705-0](https://doi.org/10.1016/S0008-8846(01)00705-0).
- 256 Konar, B. and Jung, I.-H. (2020) 'A coupled phase diagram experimental study and thermodynamic  
257 optimization of the Li<sub>2</sub>O–CaO–Al<sub>2</sub>O<sub>3</sub> and Li<sub>2</sub>O–CaO–SiO<sub>2</sub> systems, and prediction of the phase  
258 diagrams of the Li<sub>2</sub>O–CaO–Al<sub>2</sub>O<sub>3</sub>–SiO<sub>2</sub> system', *Journal of the European Ceramic Society*, 40(5), pp.  
259 2185–2199. Available at: <https://doi.org/10.1016/j.jeurceramsoc.2019.12.043>.
- 260 Korbel, C., Filippova, I.V. and Filippov, L.O. (2023) 'Froth flotation of lithium micas – A review',  
261 *Minerals Engineering*, 192, p. 107986. Available at: <https://doi.org/10.1016/j.mineng.2022.107986>.
- 262 Korkmaz, A.V. and Hacifazlıoğlu, H. (2024) 'Assessment of meta-schist as a novel sustainable resource  
263 for Portland cement manufacturing', *Advances in Cement Research*, 0(0), pp. 1–13. Available at:  
264 <https://doi.org/10.1680/jadcr.23.00132>.
- 265 Leemann, A. *et al.* (2014) 'Mitigation of ASR by the use of LiNO<sub>3</sub>—Characterization of the reaction  
266 products', *Cement and Concrete Research*, 59, pp. 73–86. Available at:  
267 <https://doi.org/10.1016/j.cemconres.2014.02.003>.
- 268 Leemann, A. *et al.* (2015) 'ASR prevention — Effect of aluminum and lithium ions on the reaction  
269 products', *Cement and Concrete Research*, 76, pp. 192–201. Available at:  
270 <https://doi.org/10.1016/j.cemconres.2015.06.002>.
- 271 Mohamed, Manel *et al.* (2022) 'Effects of partial Li-substitution on structural, electrical and dielectric  
272 properties in La<sub>1-x</sub>Li<sub>x</sub>SrMn<sub>2</sub>O<sub>5+δ</sub> (x = 0.05, 0.10 and 0.15) brownmillerite oxides', *Journal of  
273 Molecular Structure*, 1258, p. 132658. Available at: <https://doi.org/10.1016/j.molstruc.2022.132658>.

274 Panda, D., Hota, S.S. and Choudhary, R.N.P. (2023) 'A brownmillerite electronic material LiBiFe<sub>2</sub>O<sub>5</sub>:  
 275 structural, dielectric, electrical, and ferroelectric properties for device application', *Phase Transitions*,  
 276 96(11–12), pp. 822–839. Available at: <https://doi.org/10.1080/01411594.2023.2272015>.

277 Penen, F. *et al.* (2022) 'Time of Flight Secondary Ion Mass Spectrometry imaging for precise  
 278 localization of zirconium-labelled trastuzumab in xenograft cancer tumour tissues', *Microchemical*  
 279 *Journal*, 181, p. 107860. Available at: <https://doi.org/10.1016/j.microc.2022.107860>.

280 Polkonikov, V. *et al.* (2021) 'Periodic Multilayer for X-ray Spectroscopy in the Li K Range', *Applied*  
 281 *Sciences*, 11(14). Available at: <https://doi.org/10.3390/app11146385>.

282 Rahman, A. *et al.* (2015) 'Recent development on the uses of alternative fuels in cement  
 283 manufacturing process', *Fuel*, 145, pp. 84–99. Available at:  
 284 <https://doi.org/10.1016/j.fuel.2014.12.029>.

285 Scrivener, K. *et al.* (2016) 'Electron microscopy', in *A Practical Guide to Microstructural Analysis of*  
 286 *Cementitious Materials*, pp. 351–415.

287 Scrivener, K.L. (2004) 'Backscattered electron imaging of cementitious microstructures:  
 288 understanding and quantification', *Cement and Concrete Composites*, 26(8), pp. 935–945.

289 Song, Q. *et al.* (2021) 'The occurrence of MgO and its influence on properties of clinker and cement:  
 290 A review', *Construction and Building Materials*, 293, p. 123494. Available at:  
 291 <https://doi.org/10.1016/j.conbuildmat.2021.123494>.

292 Song, Z., Lu, Z. and Lai, Z. (2021) 'The effect of lithium silicate impregnation on the compressive  
 293 strength and pore structure of foam concrete', *Construction and Building Materials*, 277, p. 122316.  
 294 Available at: <https://doi.org/10.1016/j.conbuildmat.2021.122316>.

295 Spanu, G. *et al.* (2024) 'Advanced Electrode Materials Based on Brownmillerite Calcium Ferrite for Li-  
 296 Ion Batteries', *Batteries & Supercaps*, 7(8), p. e202400063. Available at:  
 297 <https://doi.org/10.1002/batt.202400063>.

298 Stutzman, P. (2004) 'Scanning electron microscopy imaging of hydraulic cement microstructure',  
 299 *Cement and Concrete Composites*, 26(8), pp. 957–966.

300 Stutzman, P. (2012) 'Microscopy of clinker and hydraulic cements', *Reviews in Mineralogy and*  
 301 *Geochemistry*, 74, pp. 101–146.

302 Sulcek, L., Marler, B. and Fechtelkord, M. (2023) 'Cation and anion ordering in synthetic lepidolites  
 303 and lithian muscovites: influence of the OH<sup>-</sup>/<sub>F</sub> and Li<sup>+</sup>/<sub>Al</sub> ratios on the mica formation studied by  
 304 NMR (nuclear magnetic resonance) spectroscopy and X-ray diffraction', *European Journal of*  
 305 *Mineralogy*, 35(2), pp. 199–217. Available at: <https://doi.org/10.5194/ejm-35-199-2023>.

306 Sweetapple, M.T. and Tassios, S. (2015) 'Laser-induced breakdown spectroscopy (LIBS) as a tool for in  
 307 situ mapping and textural interpretation of lithium in pegmatite minerals', 100(10), pp. 2141–2151.  
 308 Available at: <https://doi.org/10.2138/am-2015-5165>.

309 Teng, F.-Z. *et al.* (2004) 'Lithium isotopic composition and concentration of the upper continental  
 310 crust', *Geochimica et Cosmochimica Acta*, 68(20), pp. 4167–4178. Available at:  
 311 <https://doi.org/10.1016/j.gca.2004.03.031>.

312 Teng, F.-Z. *et al.* (2008) 'Lithium isotopic composition and concentration of the deep continental  
313 crust', *Chemical Geology*, 255(1), pp. 47–59. Available at:  
314 <https://doi.org/10.1016/j.chemgeo.2008.06.009>.

315 Thiéry, V. and Bou Farhat, H. (2023) 'Lithium-bearing minerals under the scanning electron  
316 microscope equipped with energy dispersive spectrometry: Challenges, recent advances and  
317 prospects', *Chemical Geology*, p. 121573. Available at:  
318 <https://doi.org/10.1016/j.chemgeo.2023.121573>.

319 Thiéry, V., Dubois, E. and Bellayer, S. (2022) 'The good, the bad and the ugly polishing: Effect of  
320 abrasive size on standardless EDS analysis of Portland cement clinker's calcium silicates', *Micron*, 158,  
321 pp. 103266–103266. Available at: <https://doi.org/10.1016/j.micron.2022.103266>.

322 Thiéry, V., Trincal, V. and Davy, C. (2017) 'The elusive ettringite under the high-vacuum SEM - a  
323 reflection based on natural samples, the use of Monte-Carlo modeling of EDS analyses, and an  
324 extension to the ettringite group minerals', *Journal of Microscopy*, 268, pp. 84–93.

325 Tung, N.X., Kitagaki, R. and Yamakita, Y. (2020) 'The Repairing Effects of Lithium Silicate Based  
326 Material to the Surface of Hardened Concrete', in C. Ha-Minh *et al.* (eds) *CIGOS 2019, Innovation for*  
327 *Sustainable Infrastructure*. Singapore: Springer Singapore, pp. 477–482.

328 West, A.R. (1978) 'Phase Equilibria in the System Li<sub>2</sub>O-CaO-SiO<sub>2</sub>', *Journal of the American Ceramic*  
329 *Society*, 61(3–4), pp. 152–155. Available at: <https://doi.org/10.1111/j.1151-2916.1978.tb09260.x>.

330 Witzleben, S.T. (2020) 'Acceleration of Portland cement with lithium, sodium and potassium silicates  
331 and hydroxides', *Materials Chemistry and Physics*, 243, p. 122608. Available at:  
332 <https://doi.org/10.1016/j.matchemphys.2019.122608>.

333 Woermann, E., Hahn, Th. and Eysel, W. (1979) 'The substitution of alkalis in tricalcium silicate',  
334 *Cement and Concrete Research*, 9(6), pp. 701–711. Available at: [https://doi.org/10.1016/0008-](https://doi.org/10.1016/0008-8846(79)90065-6)  
335 [8846\(79\)90065-6](https://doi.org/10.1016/0008-8846(79)90065-6).

336 Yonggang, M. and Jie, Z. (1998) 'A rheological model for lithium lubricating grease', *Tribology*  
337 *International*, 31(10), pp. 619–625. Available at: [https://doi.org/10.1016/S0301-679X\(98\)00083-8](https://doi.org/10.1016/S0301-679X(98)00083-8).

338 Zhao, H., Wang, Y. and Cheng, H. (2023) 'Recent advances in lithium extraction from lithium-bearing  
339 clay minerals', *Hydrometallurgy*, 217, p. 106025. Available at:  
340 <https://doi.org/10.1016/j.hydromet.2023.106025>.

341